Biosensors and Bioelectronics 26 (2011) 3456–3463

Contents lists available at ScienceDirect

Biosensors and Bioelectronics

journal homepage: www.elsevier.com/locate/bios

Palladium nanoparticle/chitosan-grafted graphene nanocomposites for construction of a glucose biosensor

Qiong Zeng[a], Jin-Sheng Cheng[b], Xiao-Fei Liu[a], Hao-Tian Bai[a], Jian-Hui Jiang[a,*]

[a] State Key Laboratory of Chemo/Bio-Sensing and Chemometrics, College of Chemistry and Chemical Engineering, Hunan University, Changsha 410082, Hunan, China
[b] Department of Chemistry, Key Lab of Bioorganic Phosphorus Chemistry and Chemical Biology, Tsinghua University, Beijing 100084, China

ARTICLE INFO

Article history:
Received 31 October 2010
Received in revised form 7 January 2011
Accepted 18 January 2011
Available online 25 January 2011

Keywords:
Graphene
Chitosan-grafted graphene
Palladium nanoparticles
Glucose biosensor

ABSTRACT

Graphene (GR) was covalently functionalized with chitosan (CS) to improve its biocompatibility and hydrophilicity for the preparation of biosensors. The CS-grafted GR (CS-GR) rendered water-soluble nanocomposites that were readily decorated with palladium nanoparticles (PdNPs) using in situ reduction. Results with TEM, SEM, FTIR, Raman and XRD revealed that CS was successfully grafted without destroying the structure of GR, and PdNPs were densely decorated on CS-GR sheets with no aggregation occurring. A novel glucose biosensor was then developed through covalently immobilizing glucose oxidase (GOD) on a glassy carbon electrode modified with the PdNPs/CS-GR nanocomposite film. Due to synergistic effect of PdNPs and GR, the PdNPs/CS-GR nanocomposite film exhibited excellent electrocatalytical activity toward H_2O_2 and facilitated high loading of enzymes. The biosensor demonstrated high sensitivity of 31.2 μA mM^{-1} cm^{-2} for glucose with a wide linear range from 1.0 μM to 1.0 mM as well as a low detection limit of 0.2 μM (S/N = 3). The low Michaelis–Menten constant (1.2 mM) suggested enhanced enzyme affinity to glucose. These results indicated that PdNPs/CS-GR nanocomposites held great potential for construction of a variety of electrochemical biosensors.

1. Introduction

Graphene (GR), an atomic layer of carbon atoms densely packed together in a honeycomb hexagonal lattice, is one of the few stable two-dimensional structures (Meyer et al., 2007). Because of their extraordinary electronic, optical, thermal, and mechanical properties, GR sheets hold great potential in various fields, including field effect transistors (Li et al., 2008a), electromechanical resonators (Bunch et al., 2007), polymer nanocomposites (Ramanathan et al., 2008; Vickery et al., 2009), and energy storage devices (Stoller et al., 2008; Yoo et al., 2008). Recent years also witness increasing applications of GR sheets in biosensor systems. For example, Mohanty and Berry (2008) have incorporated GR in live-bacterial-hybrid devices, DNA sensors, and polarity-specific molecular transistors, and excellent sensitivity was achieved in these devices. Postma (2010) has used GR as the electrode and the membrane material for rapid sequencing of individual DNA molecules. Nevertheless, GR sheets are hydrophobic and cannot be dispersed in most solvents (Li et al., 2008b), which may limit their biological applications due to the fact that most of their superlative properties are only associated with individual sheets. In the context, GR oxide is frequently utilized as a water-soluble alternative to GR in biosensor systems for detection of DNA and protein (Lu et al., 2009). However, oxidation disrupts the basal plane structure of GR, and the oxide sheets will exhibit inferior electronic and optic performance to GR. Our group has reported the use of surfactant to disperse GR in aqueous solution, which allows the development of a resonance energy transfer based aptasensor and an hierarchical enzyme–GR composites based enzymatic sensor (Chang et al., 2010; Zeng et al., 2010). Alternatively, water-soluble GR composites can be prepared via simple sonication processing for non-covalent adsorption of hydrophilic polymers such as sulfonated polyaniline (Bai et al., 2009), Nafion (Choi et al., 2010), and chitosan (Wang et al., 2009). Such GR composites open possibilities for the development of various biosensors. Despite of the success, long-term stability of such GR composites is difficult to be achieved because of desorption of the polymers. Efforts have been made to seek for covalent functionalization of GR sheets (Bekyarova et al., 2009; Shan et al., 2009a).

Chitosan (CS) is a linear hydrophilic polysaccharide biopolymer obtained from partial deacetylation of chitin, the second most abundant natural polymer on earth (Jenkins and Hudson, 2001). It possesses excellent film-forming ability, biocompatibility, good adhesion, non-toxicity, and susceptibility to chemical modification due to the presence of plentiful amino groups and hydroxyl groups. Based on these specific properties of CS, it is reasonable to speculate that both the hydrophilicity and biocompatibility of GR could be improved by functionalization of GR with CS, in particular, via covalent grafting strategy.

* Corresponding author. Tel.: +86 731 8821916; fax: +86 731 8821916.
E-mail address: jianhuijiang@hnu.edu.cn (J.-H. Jiang).

0956-5663/$ – see front matter © 2011 Elsevier B.V. All rights reserved.
doi:10.1016/j.bios.2011.01.024

In the present study, we report for the first time the preparation of CS-grafted GR (CS-GR), novel nanocomposites combining excellent water solubility and chemical susceptibility of CS with superb electronic performance of GR, for biosensor developments. In addition, covalent grafting can make the composites more stable and controllable (Choi et al., 2009; Salvio et al., 2009). Therefore, the resulting CS-GR nanocomposites may offer an ideal platform for the modification of biomolecules, the attachment of other nanostructured materials and the fabrication of bioelectronic devices. In order to explore the application of CS-GR in the development of electrochemical biosensors, we subsequently decorate palladium nanoparticles (PdNPs) on the CS-GR sheets to obtain PdNPs/CS-GR nanocomposites. PdNPs have been reported to be very effective in hydrogen peroxide (H_2O_2) oxidation and reduction (Lim et al., 2005). A PdNPs/CS-GR modified electrode is then prepared by casting the suspension of PdNPs/CS-GR onto a glassy carbon electrode. The resulting PdNPs/CS-GR modified glassy carbon electrode displays remarkable electrocatalytic performance toward H_2O_2. With glucose oxidase (GOD) as a model, we fabricate a glucose biosensor based on tethering the enzymes to the PdNPs/CS-GR nanocomposites via covalent crosslinking. Electrochemical measurements reveal that the glucose biosensor exhibits high sensitivity, wide linear range, low detection limit and short response time.

2. Materials and methods

2.1. Materials

Graphite powder (99.99995%, 325 mesh) and palladium chloride ($PdCl_2$) were purchased from Alfa Aesar (Ward Hill, MA, USA). Chitosan (~90% deacetylation), supplied by National Medicine Group (Shanghai, China), was ground and sieved, and the fraction <125 μm was used in our experiments. β-D-glucose, uric acid, and GOD (EC 1.1.3.4, Type X-S, lyophilized powder, 100–250 units/mg, from Aspergillus niger) were purchased from Sigma–Aldrich (St. Louis, MO, USA). Other chemicals were obtained as analytical-grade products from Beijing Chemical Company (Beijing, China). All aqueous solutions were prepared using deionized water using a Millipore water purification system with a minimum resistivity of 18.0 MΩ cm.

2.2. Apparatus and measurements

Transmission electron microscopy (TEM) analysis was performed using JEOL JEM 1200EX electron microscope, and high-resolution TEM analysis was conducted using JEOL JEM 2010 electron microscope at an accelerating voltage of 100 kV. Scanning electron microscopy (SEM) images were obtained by using JSM-7401 scanning electron microscopy operating. Fourier transform infrared spectroscopy (FTIR) was recorded on a Spectrum One (PerkinElmer) spectrometer with a resolution of 4 cm^{-1}. Raman spectroscopy (Renishaw microprobe RM1000) was recorded at a wavelength of 633 nm (He–Ne laser). Powder X-ray diffraction (XRD) studies of the PdNPs/CS-GR nanocomposites were performed on a Bruker D8 Advance X-ray powder diffractometer (CuKa radiation, λ = 1.5406 Å). Cyclic voltammetry, electrochemical impedance spectroscopy (EIS), and amperometry were performed using a CHI 760B electrochemical workstation (CH Instruments Inc., USA). The electrochemical measurements were based on a conventional three-electrode system with a saturated calomel electrode (SCE) as the reference electrode, a platinum foil electrode as the counter electrode and the modified glassy carbon electrode (GCE, 4 mm diameter) as the working electrode. EIS measurements were performed in the presence of 5 mM $K_3[Fe(CN)_6]$ and 1 M KCl. The amperometric measurements in response to H_2O_2 and glucose were performed at an applied potential of +0.7 V in 0.05 M phosphate buffer (PB, pH 7.5) under stirring at room temperature (25 ± 1 °C).

2.3. Preparation of CS-GR and PdNPs/CS-GR

GR oxide was prepared by a modified Hummers method (Hummers and Offeman, 1958; Li et al., 2009; Tang et al., 2009). The obtained GR oxide (200 mg) was refluxed in $SOCl_2$ (40 mL) for 52 h to give the intermediate GR oxide–COCl (219.2 mg). Phthaloyl chitosan was synthesis according to a documented procedure (Kurita et al., 2002). In a typical experiment, phthaloyl chitosan (1.753 g) and LiCl (1.201 g) were dispersed in dimethylacetamide (120 mL), and the mixture was stirred at 140 °C for 2 h, then GR oxide–COCl (219.2 mg) was added with the addition of 14.0 mL pyridine followed. The mixture was refluxed under nitrogen for 48 h, and the resultant mixture was filtered, washed, and vacuum-dried. The obtained powder (205 mg) was dispersed in hydrazine hydrate (15 mL) at 80 °C for 16 h. After the reaction, the mixture was filtered, washed with ethanol and deionized water followed by vacuum-drying for 24 h, producing the CS-GR composites (175 mg). (*Note:* Oxygen-containing functional groups in GR oxide, such as carboxylic, epoxyl, and hydroxylic groups, could be mostly reduced during the synthesis (Stankovich et al., 2007; Tang et al., 2009)). The obtained CS-GR (175 mg) was suspended in a mixture of H_2O (2.6 mL) and ethylene glycol (18 mL). After sonication, palladium chloride in ethylene glycol solution (18 mL, 2.03 mg Pd/mL) was added dropwisely (Li et al., 2003). With the pH value of the mixture adjusted to 5 using HCl (0.1 M), the mixture was stirred overnight to allow in situ decoration of PdNPs on CS-GR composites. Subsequently, the mixture was treated with NaOH solution (2.5 M, in ethylene glycol) to adjust the pH to 13, followed by heating at 140 °C for 3 h under flowing N_2. After cooling, the mixture was filtered through a 0.2 μm PTFE membrane filter, washed extensively with ethanol and deionized water, and dried under vacuum at 65 °C for 24 h to yield the PdNPs/CS-GR nanocomposites with plentiful amino groups for further modification (196.3 mg).

2.4. Construction of PdNPs/CS-GR modified electrode and glucose biosensor

Prior to coating, GC electrodes were polished with 1, 0.3, and 0.05 μm α-alumina slurries successively and sonicated with deionized water. 2 mg PdNPs/CS-GR nanocomposites were dispersed in 1 mL of 5% acetic acid aqueous solution under sonication. An aliquot of 8 μL of the resulting PdNPs/CS-GR suspension was dropped on the surface of a glassy carbon electrode, and dried slowly to obtain the PdNPs/CS-GR modified electrode.

The PdNPs/CS-GR modified electrode was immersed in the 0.5% glutaric dialdehyde solution for 1 h at room temperature, and rinsed with deionized water followed by drying in air. 8 μL of 4 mg/mL GOD solution was then dropped on the surface of the modified electrode and dried at 4 °C. The resulting GOD-immobilized electrode was then soaked in 0.05 M phosphate buffer (PB, pH 7.5) for 20 min to remove loosely adsorbed GOD. The as-prepared glucose biosensor was stored at 4 °C in 0.05 M PB (pH 7.5) in a refrigerator when not in use.

3. Results and discussion

3.1. Characterization of CS-GR, and PdNPs/CS-GR nanocomposites

The CS is covalently grafted to GR through the reaction of carboxyl groups on GR oxides with hydroxyl groups on CS to form ester linkages. PdNPs/CS-GR nanocomposites are synthesized through in situ reduction reaction in the mixture of Pd salt and CS-GR using

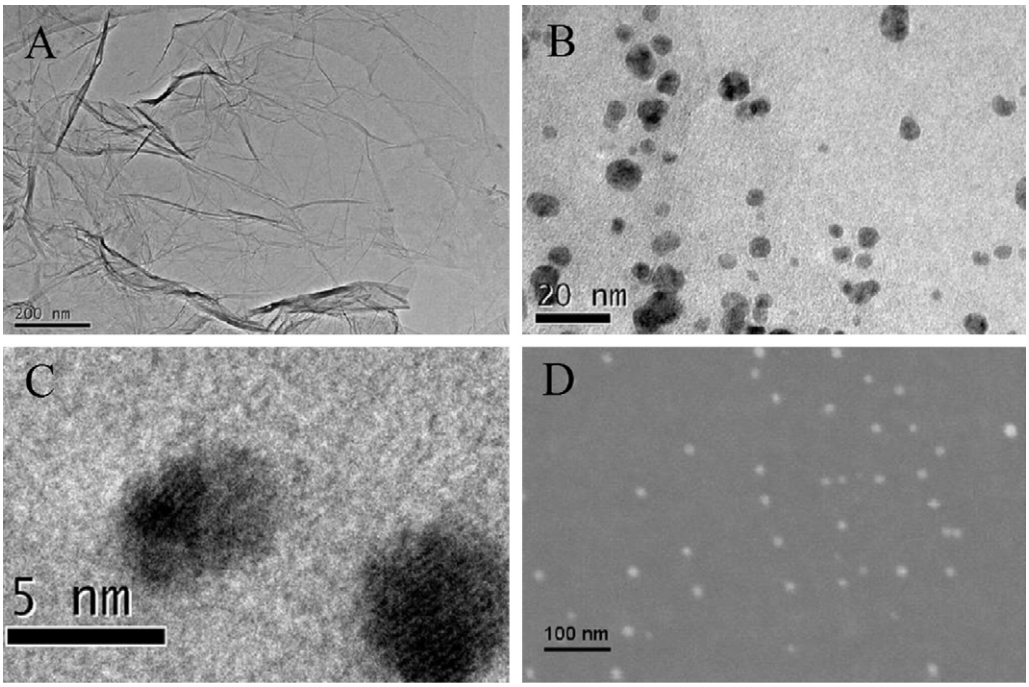

Fig. 1. (A) TEM image of CS-GR, (B and C) HRTEM images of PdNPs/CS-GR and (D) SEM image of PdNPs/CS-GR.

ethylene glycol as the reductant. The CS-GR and PdNPs/CS-GR are both observed to show adequate solubility and long-term stability in 5% acetic acid aqueous solution, indicating that effective dispersion of GR is achieved by covalently grafting CS to GR.

The TEM image (Fig. 1A) displays a view of CS-GR nanosheets, clearly illustrating typical flake-like wrinkled shapes of GR. A direct evidence for the attachment of PdNPs to the CS-GR surface is given by the high-resolution TEM (HRTEM) tests. A typical HRTEM image is shown in Fig. 1B. It is observed that PdNPs are densely decorated on the surface of CS-GR. These nanoparticles are well separated, appeared spherical in shape, and give a diameter range of 2–9 nm with the majority centered at 4–5 nm. A higher magnification of HRTEM in Fig. 1C clearly reveals the lattice planes of Pd, indicating the polycrystalline nature of PdNPs. SEM image shown in Fig. 1D further confirms the effective deposition of PdNPs on CS-GR with a narrow particle size distribution. Note that to fully utilize the electrocatalytic property of PdNPs, it is very important to decorate them on the CS-GR in a dense and well-dispersed way. It has been reported that the surface groups of carbon such as carboxyl, hydroxyl, and carbonyl groups, which act as anchoring sites for metal ions used for forming the nanoparticles, are crucial for deposition of metal nanoparticles on carbon nanotubes (CNTs) (Yu et al., 1998). Therefore, the chemical functional groups, such as amine in the CS-GR composites are also beneficial to anchor palladium ions, which thus serve an excellent substrate for the formation of PdNPs with high catalytic activity on the surface of CS-GR.

Further evidences supporting the synthesis of CS-GR and PdNPs/CS-GR nanocomposites are supplied by FTIR and XRD. From the FTIR spectra in Fig. 2, a characteristic peak of GR is observed at 1545 cm^{-1} on curves b–d, which is assigned to the skeletal vibrations. The spectrum of CS-GR, curve c, displays two characteristic bands of the glucopyranose rings at 890 and 1150 cm^{-1}, respectively, implying the grafting of CS on GR (Mi, 2005). Comparing CS-GR and PdNPs/CS-GR, it is clear that the C–O ester feature from 1000 to 1200 cm^{-1} becomes a broad band centered at 1044 cm^{-1}, manifesting strong interactions between PdNPs and the ester O (Hull et al., 2006).

From the XRD patterns in Fig. 3, it is observed that CS-GR nanosheets give a characteristic peak at $2\theta = 24.7^{\circ}$ (curve a), which is the same as that of GR (Wang et al., 2009), confirming that the CS-GR composites still retain the structure of GR. A major characteristic peak of Pd (1 1 1) is obtained at 39.6° on curve b, suggesting successful reduction of palladium ion to Pd (0). The other two peaks at 45.5 ° and 67.3° are attributed to (2 0 0) and (2 2 0) crystalline plane diffraction peaks of Pd (0).

The structures of CS-GR and PdNPs/CS-GR are further investigated using Raman spectroscopy (Fig. S1 in Supplementary Materials). In the Raman spectra of CS-GR and PdNPs/CS-GR two characteristic bands are obtained near 1332 and 1594 cm^{-1}, similarly to that in GR. This gives immediate evidence that the covalent functionalization of GR with CS and the decoration of PdNPs onto CS-GR do not disrupt the unique π-electronic network of GR. Therefore, it is expected that CS-GR and PdNPs/CS-GR will also exhibit superb electronic and optic performance of GR.

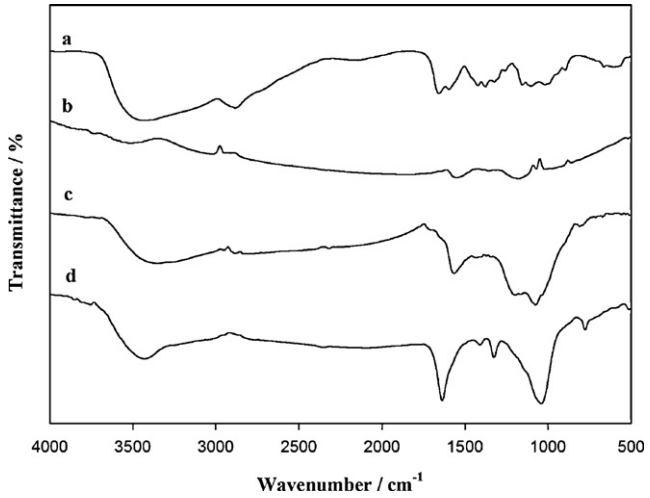

Fig. 2. FTIR spectra of (a) CS, (b) GR, (c) CS-GR, and (d) PdNPs/CS-GR.

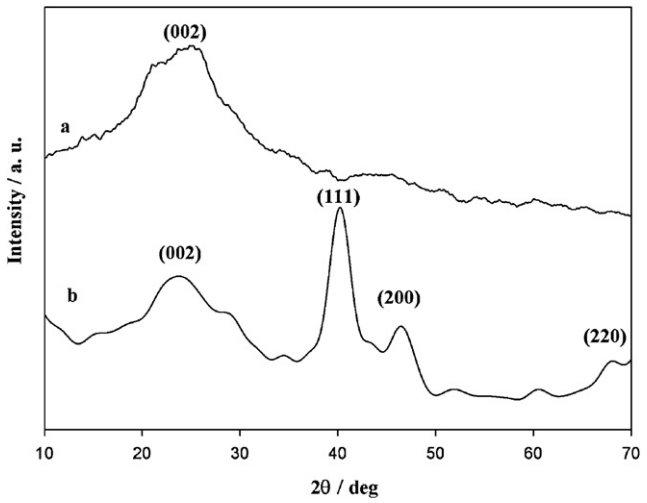

Fig. 3. XRD patterns of (a) CS-GR, and (b) PdNPs/CS-GR.

3.2. Characterization of the modified electrodes

Because CS-GR combines excellent water solubility and chemical susceptibility of CS with superb electronic performance of GR, it may find potential in the development of electrochemical biosensors. Prior to the implementation of the CS-GR-based biosensor, we firstly investigate the electrochemical behavior of the PdNPs/CS-GR modified electrode using cyclic voltammetry and electrochemical impedance spectroscopy with $K_3Fe(CN)_6$ as the redox probe. Fig. 4A depicts typical cyclic voltammograms of the PdNPs/CS-GR modified electrode in 5 mM $K_3Fe(CN)_6$ and 1 M KCl at different scan rates. One observes that the potentials and peak currents for the $[Fe(CN)_6]^{3-/4-}$ redox processes (anodic and cathodic) show strong dependency upon the scan rates. The peak-to-peak separation becomes slightly widened with increasing scan rate. At the scan rate ranging from 20 to 1000 mV/s, both the anodic and the cathodic peak currents increase linearly with the square root of the scan rates (correlation coefficients of 0.997 and 0.996 for anodic and cathodic peaks, respectively), suggesting that the reaction is diffusion controlled (Fig. 4B).

EIS is used to investigate the interfacial changes of the electrode surface during the fabrication process (Fig. S2 in Supplementary Materials). A very slight increase in electrochemical impedance is obtained after the CS-GR coating, indicator of excellent conductivity of the CS-GR composites. Obvious increase in electrochemical impedance is observed after the modification with PdNPs/CS-GR, which may be originated from the increased electron transfer resistance of PdNPs, negatively charged NPs, to negatively charged $Fe(CN)_6^{3-/4-}$. The electron transfer resistance for GOD/PdNPs/CS-GR/GCE is even higher than that of PdNPs/CS-GR/GCE, which seems attributed to the hindrance of electron-transfer kinetics by immobilized GOD molecules. This implies the successful immobilization of GOD on the electrode. SEM characterization of the electrode surfaces is also performed (Fig. S3 in Supplementary Materials). It is observed that these modified electrodes all show very rough morphologies, typical for nanocomposites modified surfaces. Also, with the immobilization of PdNPs and GOD molecules, typical white dots corresponding to these NPs or proteins are observed, confirming the successful immobilization of PdNPs and GOD on the electrode.

3.3. Electrocatalytic effect toward H_2O_2 of the modified electrodes

Fig. 5A shows the cyclic voltammograms of 0.5 mM H_2O_2 at bare GCE, CS-GR modified electrode, and PdNPs/CS-GR modified

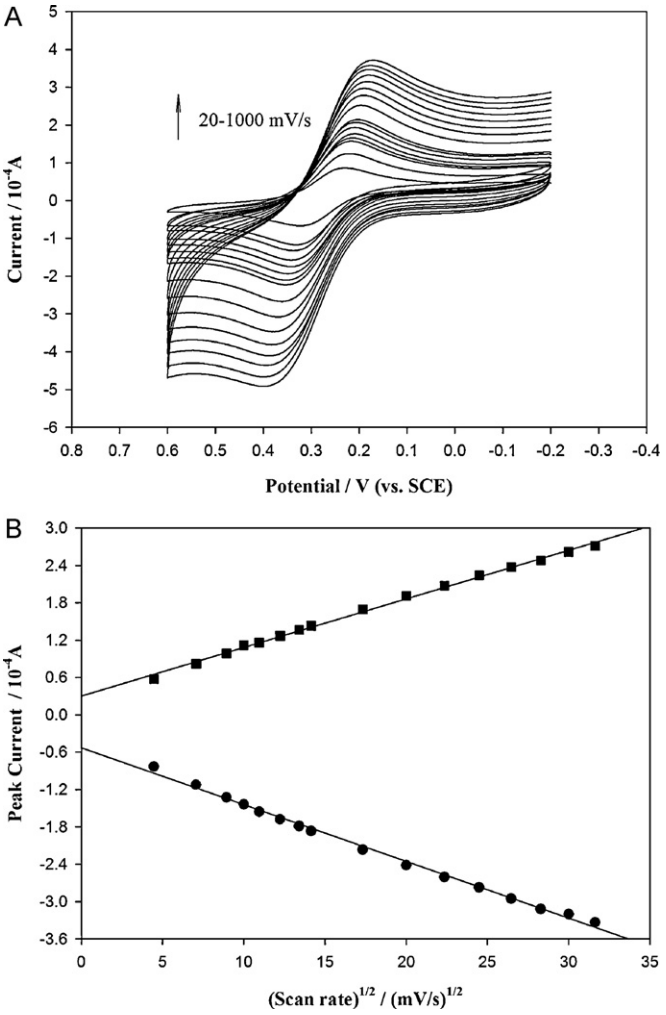

Fig. 4. (A) Cyclic voltammograms of PdNPs/CS-GR modified electrode in 5 mM $K_3Fe(CN)_6$ and 1 M KCl at scan rates of 20, 50, 80, 100, 120, 150, 180, 200, 300, 400, 500, 600, 700, 800, 900, and 1000 mV/s, respectively. (B) Plots of peak current versus the square root of the scan rate.

electrode in 0.05 mM PB at a scan rate of 100 mV/s. The PdNPs/CS-GR modified electrode exhibits stronger oxidation current of H_2O_2 with increasing potential applied on the electrode. Hence, in order to have desirable sensitivity, we select the working potential as 0.7 V in subsequent experiments.

Fig. 5B shows typical amperometric responses at potential of 0.7 V to increasing levels of H_2O_2 in 0.08 mM each step on the bare GCE, CS-GR modified electrode, and the PdNPs/CS-GR modified electrode. It is seen that the bare GCE and CS-GR modified electrode only displays slight increases in current in response to successive additions of H_2O_2. In contrast, the PdNPs/CS-GR modified electrode exhibits appreciable increases in current in response to successive additions of H_2O_2. Such excellent catalytic activity of the PdNPs/CS-GR modified electrode may be attributed to the synergistic effect of GR and PdNPs. The electrode reaches 95% of the steady-state current within 5 s. Such fast and sensitive response may be arising from the ease in diffusion of H_2O_2 from external solution into the nanocomposite film. Reproducibility of the electrode was also satisfactory. The relative standard deviation (RSD) of ten repetitive measurements of 0.08 mM H_2O_2 is ~4.5%, confirming the operational stability of the nanocomposite film. In addition, the RSD of current signals for the measurement of 0.08 mM H_2O_2 at five modified electrodes fabricated in parallel is 4.7%, which proves acceptable reproducibility in elec-

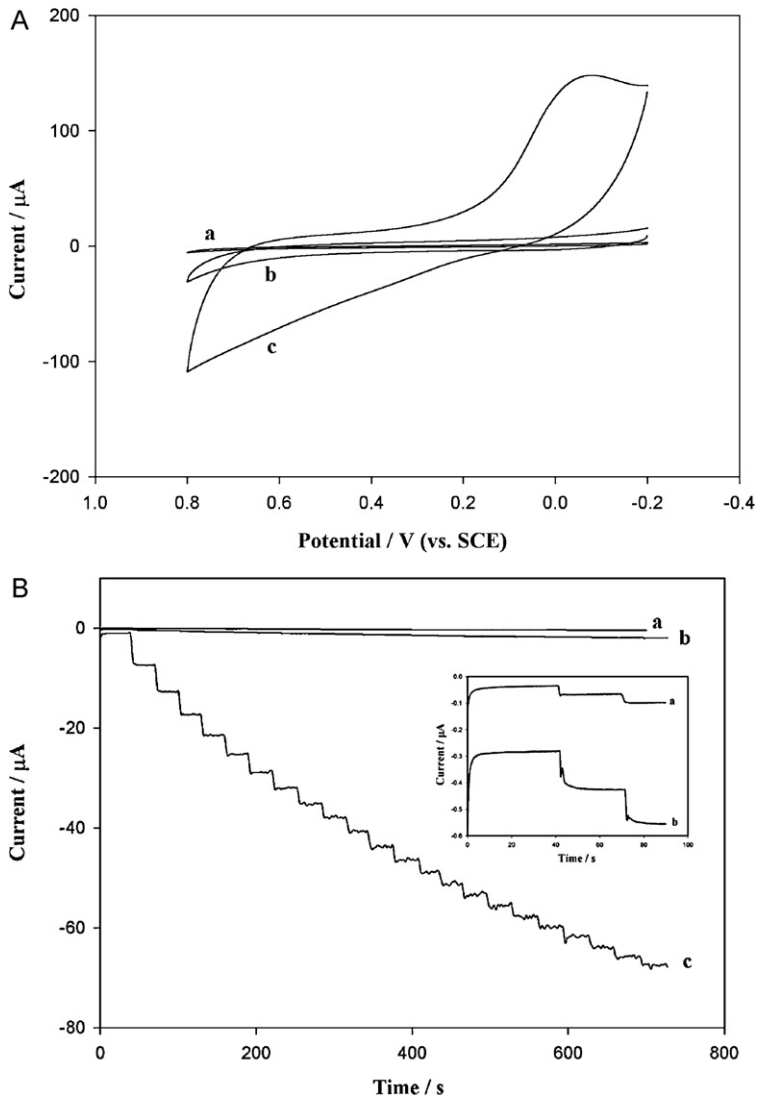

Fig. 5. (A) Cyclic voltammograms of (a) bare GCE (b) CS-GR, and (c) PdNPs/CS-GR modified electrodes in 0.05 M PB (pH 7.5) at a scan rate of 100 mV s^{-1} in the presence of 0.5 mM H_2O_2. (B) Amperometric responses of (a) bare GCE, (b) CS-GR, and (c) PdNPs/CS-GR modified electrodes upon successive addition of 0.08 mM H_2O_2 solution in 0.05 M PB (pH 7.5) at +0.7 V.

trode fabrication. Because the PdNPs decorated on the surface of CS-GR are well separated and densely loaded on excellent electron-conducting nanosheets, they offer a large active surface and enhance the electrocatalytic activity toward H_2O_2. As a result, the PdNPs/CS-GR modified electrode displays high electrocatalytic activity toward H_2O_2, fast electron-transfer kinetics, and good reproducibility, which implies that the electrode represents an ideal platform for developing oxidase-based electrochemical biosensors.

3.4. Optimization of experimental variables

The biosensor, i.e. the GOD/PdNPs/CS-GR modified electrode, was fabricated by incorporating GOD into the PdNPs/CS-GR nanocomposites film through glutaric dialdehyde. Immobilization of GOD using covalent conjugation can achieve a glucose biosensor with better stability. The principle of the biosensor is based on the amperometric detection of H_2O_2, which is produced during the GOD-catalyzed oxidation of glucose in the presence of dissolved oxygen. The mechanism for the detection of glucose is given by the following reactions:

$$\text{D-glucose} + O_2 + H_2O \xrightarrow{\text{GOD}} \text{D-gluconicacid} + H_2O_2$$

$$H_2O_2 \rightarrow 2H^+ + O_2 + 2e^-$$

The H_2O_2 generated in this reaction can be electrochemically oxidized at the conductive GR and PdNPs surfaces, producing a redox current that is proportional to the concentration of glucose in the stock sample.

The solution acidity is an important factor influencing the performance of the enzyme electrode, since the bioactivity of the immobilized GOD is pH-dependent. The current response of the GOD/PdNPs/CS-GR modified electrode to 0.08 mM glucose increases in the pH range of 5.5–7.5, and decreased at higher pH values (Fig. S4 in Supplementary Materials). The decrease of current response at strong acidic and alkaline solution might be originated from the decrease in bioactivity of the enzyme. Maximum current is obtained at pH 7.5, which is near the physiological condition and is chosen for subsequent experiments.

Further optimization of experimental conditions such as the amount of PdNPs/CS-GR and the amount of GOD in preparing the

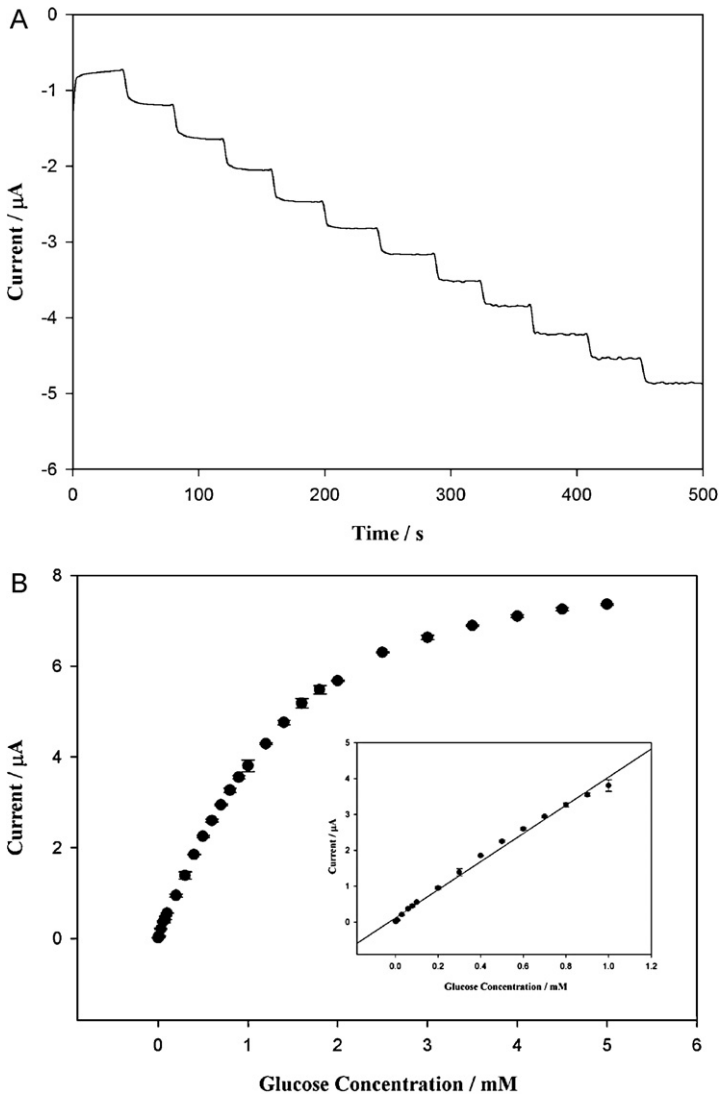

Fig. 6. (A) Amperometric responses for GOD/PdNPs/CS-GR modified electrode upon successive addition of 0.08 mM glucose solution in 0.05 M PB (pH 7.5) at +0.7 V. (B) Calibration curve of the enzyme electrode corresponding to amperometric response at +0.7 V. Error bars are the SD of four repetitive experiments. The average relative SD is 3.7%. Inset is the linear range of the calibration curve. The average relative SD is 3.5%.

biosensor is performed. The biosensor exhibits the highest sensitivity to glucose when the amount of PdNPs/CS-GR (2 mg/mL) is 8 μL (Fig. S5 in Supplementary Materials). Smaller amount of PdNPs/CS-GR gives lower sensitivity, possibly due to decreased loading of enzyme molecules. In contrast, when the amount of PdNPs/CS-GR is too large, the electrode may show very high electrochemical impedance, thus lowering the sensitivity and prolonging the response time. The GOD loading is also found to have substantial effect on amperometric response of the biosensor toward 0.08 mM glucose (Fig. S6 in Supplementary Materials). The maximum current is obtained at 4 mg/mL of GOD loading. Therefore, 4 mg/mL of GOD is adopted to prepare the biosensor.

3.5. Determination of glucose at GOD/PdNPs/CS-GR modified electrode

The cyclic voltammograms of the modified GCEs with GOD/CS, GOD/CS-GR, and GOD/PdNPs/CS-GR films are investigated in 0.05 M PB (pH 7.5) at a scan rate of 50 mV s^{-1} in the presence of 0.8 mM glucose (Fig. S7 in Supplementary Materials). For GOD/CS-GR and GOD/CS modified electrodes, no appreciable current peaks appear in the cyclic voltammograms, indicating that these modifications have little catalytic activity. In contrast, a pair of strong current peaks are obtained at the GOD/PdNPs/CS-GR modified electrode, demonstrating desirable catalytic activity and biocompatibility of the PdNPs/CS-GR nanocomposites.

Fig. 6A displays typical chronoamperometric responses of the biosensor of successive additions of 0.08 mM glucose at an applied potential of +0.7 V. The enzyme electrode exhibits excellent electrocatalytic activity for glucose detection with steep increases in current responses, and the time required to reach 95% of the steady-state current is less than 10 s. This result indicates that the biosensor shows very sensitive and rapid response characteristics. This might be due to the fact that GR nanosheets are highly electron-conductive, which provides a low-resistance pathway between glucose and the immobilized GOD, facilitating the electron transfer and reducing the response time.

Fig. 6B depicts the calibration curve of the biosensor. The inset illustrates the linear response range of the biosensor to glucose concentration, which spans from 1.0 μM to 1.0 mM with a correlation coefficient of 0.991. A low detection limit of 0.2 μM is readily achieved at a signal-to-noise ratio of 3.

The performance of the developed glucose biosensors is compared with some of existing sensors based on carbon nanoma-

Table 1
Construction and performance of some glucose biosensors based on carbon nanomaterials (as one of the component in the matrix for enzyme immobilization).

Glucose biosensor	Protocol	Linear range (mM)	Detection limit (μM)	Sensitivity ($\mu A\,mM^{-1}\,cm^{-2}$)	K_m^{app} (mM)	Reference
GOD/PdNPs/CS-GR/GC	Crosslinking	0.001–1	0.2	31.2	1.2	Present work
GOD/Ptnano/SWCNT/Nafion/GC	Crosslinking	0.0005–5	0.5	30	–	Hrapovic et al. (2004)
GOD/GR/PFIL/GC	Drop-coating	2–14	–	–	–	Shan et al. (2009b)
GOD/AuNPs/GR/CS/Au	Drop-coating	2–14	180	–	–	Shan et al. (2010)
GOD/GR/CS/GC	Drop-coating	0.08–12	20	37.93	4.4	Kang et al. (2009)
GOD/PdNPs/CNT/Nafion/GC	Electrodeposition	Up to 12	150	–	–	Lim et al. (2005)
GOD/CS/CNT/Au	Electrodeposition	0.005–8	2	6.7	6.8	Zhou et al. (2007)
PDDA/GOD/PDDA/CNT/GC	Self-assembling	0.015–6	7	–	–	Liu and Lin (2006)
GOD/SWCNHs/GC	Drop-coating	0–6	6	15.00	8.5	Liu et al. (2008)
GOD/PtNPs/CNT/Nafion/GC	Drop-coating	0.16-11.5	55	–	2.6	Wen et al. (2009)
GOD/CNx-MWNTs/Nafion/GC	Drop-coating	0.02–1.02	10	13.0	2.2	Deng et al. (2009)
$(GOD/AuNPs/MWCNTs)_9/Pt$	Layer-by-layer assembling	0.1–10	6.7	35.77	14.9	Wu et al. (2007)
$\{GOD/Au\text{-}(SH)PANI\text{-}g\text{-}MWNT\}_{10}/ITO$	Layer-by-layer assembling	1–9	0.06	–	–	Komathi et al. (2009)

terials, as shown in Table 1. It is found that the developed biosensor is among the top list of biosensors with wider linear range, lower detection limit, and higher sensitivity. Such high sensitivity and wide linear range of this biosensor may be attributed to a number of factors: first, the small size, high loading and large surface area of PdNPs can enhance the performance in the peroxide oxidation process. The large surface area also facilitates substrate–enzyme contact and thus contributes to the wider linear range. Second, the biocompatible CS and GR are suitable for maintaining the nature configuration and bioactivity of GOD. Third, a large amount of enzyme can be stably immobilized on the PdNPs/CS-GR nanocomposites due to the presence of abundant amine groups in CS.

When glucose concentration is high, a plateau current is observed, typical characteristics of Michaelis–Menten kinetics. The apparent Michaelis–Menten constant (K_m^{app}), an indicator of the enzyme–substrate kinetics, can be calculated from the Lineweaver–Burk equation (Kamin and Wilson, 1980).

$$\frac{1}{i_{as}} = \frac{K_m^{app}}{i_{mas}}\frac{1}{C} + \frac{1}{i_{max}}$$

where i_{ss} is the steady-state current, i_{max} is the maximum current measured under saturated substrate condition, and C is the concentration of substrate. Using the slope and intercept from Lineweaver–Burk plot (Fig. S8 in Supplementary Materials), we estimate the value of K_m^{app} for the GOD/PdNPs/CS-GR modified electrode as 1.2 mM. Such a small K_m^{app} value may be attributed to excellent performance of CS-GR nanocomposites for high loading of enzymes and efficiently maintaining of enzymatic activity.

3.6. Reproducibility and stability of the GOD/PdNPs/CS-GR modified electrode

The operational reproducibility of the enzyme electrode has been examined. It is observed that the responses to 0.08 mM glucose give a RSD of 3.8% in ten successive measurements. The reproducibility of enzyme electrode construction is evaluated at five electrodes separately prepared under the same conditions. The results reveal that the biosensor has acceptable reproducibility with a RSD of 5.1%.

The stability of the biosensor is estimated by measuring the amperometric response for 0.08 mM glucose. It has been found that the biosensor retained about 91% of its original response after 60 times uninterrupted detection. When stored in 0.05 M pH 7.5 PB at 4 °C and measured at intervals of one week, the biosensor retains 94% of its original sensitivity after one week. After 3 weeks, the current response of the biosensor still maintains 80% of its original current response. This reveals that the covalent functionalization of graphene and covalent immobilization of GOD ensures well stability of the biosensor, preventing graphene and GOD from leaking from the PdNPs/CS-GR nanocomposites. With the help of PdNPs/CS-GR film, GOD can maintain bioactivity on the modified electrode.

3.7. Additional studies of interferences and real samples

Oxidizable compounds such as ascorbic acid and uric acid usually co-exist with glucose in real samples and may cause interferences on glucose detection. The concentration of ascorbic acid and uric acid, if considered at upper limits, are ~14 μM and ~455 μM, respectively, in human blood (Choi et al., 2002). Therefore, the interfering effects of 0.2 mM ascorbic acid and 0.5 mM uric acid are examined with reference to 5 mM glucose. The interferences of ascorbic acid and uric acid are observed to be significant at 0.7 V. However, using a potential of −0.05 V, the interferences of both interfering substances are found to be insignificant, though the sensitivity of the enzyme electrode to glucose is slightly decreased (~93%). Therefore, in subsequent real sample analysis, the working potential is chosen to be −0.05 V.

The enzyme electrode is further employed for glucose assay in five human plasma samples at the potential of −0.05 V. The blood samples are 50-fold diluted with 0.05 M PB (pH 7.5) prior to the measurements, and each sample is analyzed using standard addition method with three times addition of a standard glucose solution. The results (Table S1 in Supplementary Materials) show that the biosensor gives recoveries in the range of 92.5–105.3%, indicating the developed electrode may hold potential in real sample analysis.

4. Conclusion

In the present study, GR was covalently functionalized with CS to improve its hydrophilicity and biocompatibility without the loss of electronic performance. PdNPs/CS-GR were then synthesized by in situ reduction using the mixture of Pd salt and CS-GR. It was observed that PdNPs were well dispersed and densely decorated on CS-GR nanosheets. The PdNPs/CS-GR nanocomposites modified electrode showed high electrocatalytic activity toward the oxidation of H_2O_2. With GOD as a model oxidase enzyme, we constructed a glucose biosensor through covalent immobilization of the enzyme on the PdNPs/CS-GR nanocomposites. Amperometric responses revealed that the developed glucose biosensor had high sensitivity, wide linear range, low detection limit and good reproducibility. These desirable results indicated that the PdNPs/CS-GR nanocomposites could be a promising option for the development of various oxidase-based biosensors and bioelectronic devices.

Acknowledgements

This work was supported by NSFC (20975023, 20875027, J0830415) and Program for Changjiang Scholors and Innovative Research Team in Universities (PCSIRT) and National Grand Program on Key Infectious Disease (2009ZX10004-312).

Appendix A. Supplementary data

Supplementary data associated with this article can be found, in the online version, at doi:10.1016/j.bios.2011.01.024.

References

Bai, H., Xu, Y.X., Zhao, L., Li, C., Shi, G.Q., 2009. Chem. Commun., 1667–1669.
Bekyarova, E., Itkis, M.E., Ramesh, P., Berger, C., Sprinkle, M., Heer, W.A., Haddon, R.C., 2009. J. Am. Chem. Soc. 131, 1336–1337.
Bunch, J.S., Zande, A.M., Verbridge, S.S., Frank, I.M., Tanenbaum, D.M., Parpia, J.M., Graighead, H.G., McEuen, P.L., 2007. Science 315, 490–493.
Chang, H.X., Tang, L.H., Wang, Y., Jiang, J.H., Li, J.H., 2010. Anal. Chem. 82, 2341–2346.
Choi, B.G., Park, H.S., Park, T.J., Yang, M.H., Kim, J.S., Jang, S.Y., Heo, N.S., Lee, S.Y., Kong, J., Hong, W.H., 2010. ACS Nano 4, 2910–2918.
Choi, J.H., Kim, K.J., Kim, B.S., Lee, H.G., Kim, S.H., 2009. J. Phys. Chem. C 113, 9433–9435.
Choi, S.H., Lee, S.D., Shin, J.H., Ha, J., Nam, H., Cha, G.S., 2002. Anal. Chim. Acta 461, 251–260.
Deng, S.Y., Jian, G.Q., Lei, J.P., Hu, Z., Ju, H.X., 2009. Biosens. Bioelectron. 25, 373–377.
Hrapovic, S., Liu, Y.L., Male, K.B., Luong, J.H., 2004. Anal. Chem. 76, 1083–1088.
Hull, R.V., Li, L., Xing, Y.C., Chu, C.C., 2006. Chem. Mater. 18, 1780–1788.
Hummers, W., Offeman, R.E., 1958. J. Am. Chem. Soc. 80, 1339–11339.
Jenkins, D.W., Hudson, S.M., 2001. Chem. Rev. 101, 3245–3274.
Kamin, R.A., Wilson, G.S., 1980. Anal. Chem. 52, 1198–1205.
Kang, X.H., Wang, J., Wu, H., Aksayc, I.A., Liu, J., Lin, Y.H., 2009. Biosens. Bioelectron. 25, 901–905.
Komathi, S., Gopalan, A.I., Lee, K.P., 2009. Biosens. Bioelectron. 24, 3131–3134.
Kurita, K., Ikeda, H., Yoshida, Y., Shimojoh, M., Harata, M., 2002. Biomacromolecules 3, 1–4.
Li, D., Muller, M.B., Gilje, S., Kaner, R.B., Wallace, G.G., 2008a. Nat. Nanotechnol. 3, 101–105.
Lim, S.H., Wei, J., Lin, J.Y., Li, Q.T., You, J.K., 2005. Biosens. Bioelectron. 20, 2341–2346.
Liu, G.D., Lin, Y.H., 2006. Electrochem. Commun. 8, 251–256.
Liu, X.Q., Shi, L.H., Niu, W.X., Li, H.J., Xu, G.B., 2008. Biosens. Bioelectron. 23, 1887–1890.
Li, W.Z., Liang, C.H., Zhou, W.J., Qiu, J.S., Sun, G.Q., Xin, Q.J., 2003. J. Phys. Chem. B 107, 6292–6299.
Li, X., Wang, X., Zhang, L., Lee, S., Dai, H., 2008b. Science 319, 1229–1232.
Li, Y.M., Tang, L.H., Li, J.H., 2009. Electrochem. Commun. 11, 846–849.
Lu, C.H., Yang, H.H., Zhu, C.L., Chen, X., Chen, G.N., 2009. Angew. Chem., Int. Ed. 48, 4785–4787.
Meyer, J.C., Geim, A.K., Katsnelson, M.I., Novoselov, K.S., Booth, T.J., Roth, S., 2007. Nature 446, 60–63.
Mi, F.L., 2005. Biomacromolecules 6, 975–987.
Mohanty, N., Berry, V., 2008. Nano Lett 8, 4469–4476.
Postma, H.W., 2010. Nano Lett 10, 420–425.
Ramanathan, T., Abdala, A.A., Stankovich, S., Dikin, D.A., Alonso, M.H., Piner, R.D., Adamson, D.H., Schniepp, H.C., Chen, X., Ruoff, R.S., Nguyen, S.T., Aksay, I.A., Homme, P.K., Brinson, L.C., 2008. Nat. Nanotechnol. 3, 327–331.
Salvio, R., Krabbenborg, S., Naber, W.J., Velders, A.H., Reinhoudt, D.N., Wiel, W.G., 2009. Chem. Eur. J. 15, 8235–8240.
Shan, C.S., Yang, H.F., Han, D.X., Zhang, Q.X., Ivaska, A., Niu, L., 2010. Biosens. Bioelectron. 25, 1070–1074.
Shan, C.S., Yang, H.F., Han, D.X., Zhang, Q.X., Ivaska, A., Niu, L., 2009a. Langmuir 25, 12030–12033.
Shan, C.S., Yang, H.F., Song, J.F., Han, D.X., Ivaska, A., Niu, L., 2009b. Anal. Chem. 81, 2378–2382.
Stankovich, S., Dikin, D.A., Piner, R.D., Kohlhaas, K.A., Kleinhammes, A., Jia, Y., Wu, Y., Nguyen, S.T., Ruoff, R.S., 2007. Carbon 45, 1558–1565.
Stoller, M.D., Park, S., Zhu, Y., An, J.H., Ruoff, R.S., 2008. Nano Lett 8, 3498–3502.
Tang, L.H., Wang, Y., Li, Y.M., Feng, H.B., Lu, J., Li, J.H., 2009. Adv. Funct. Mater. 19, 2782–2789.
Vickery, J.L., Patil, A.J., Mann, S., 2009. Adv. Mater. 21, 2180–2184.
Wang, Y., Li, Y.M., Tang, L.H., Lu, J., Li, J.H., 2009. Electrochem. Commun. 11, 889–892.
Wen, Z.H., Ci, S.Q., Li, J.H., 2009. J. Phys. Chem. C 113, 13482–13487.
Wu, B.Y., Hou, S.H., Yin, F., Zhao, Z.X., Wang, Y.Y., Wang, X.S., Chen, Q., 2007. Biosens. Bioelectron. 22, 2854–2860.
Yoo, E.J., Kim, J., Hosono, E., Zhou, H.S., Kudo, T., Honma, I., 2008. Nano Lett 8, 2277–2282.
Yu, R.Q., Chen, L.W., Liu, Q.P., Lin, J.Y., Tan, K.L., Ng, S.C., Chan, H.S., Xu, G.Q., Andy, T.S., 1998. Chem. Mater. 10, 718–722.
Zeng, Q., Cheng, J.S., Tang, L.H., Liu, X.F., Liu, Y.Z., Li, J.H., Jiang, J.H., 2010. Adv. Funct. Mater. 20, 3366–3372.
Zhou, Q.M., Xie, Q.J., Fu, Y.C., Su, Z.H., Jia, X.E., Yao, S.Z., 2007. J. Phys. Chem. B 111, 11276–11284.